SOFT ROBOTICS
Volume 10, Number 3, 2023

DOI: 10.1089/soro.2022.0027

SoRo
Soft Robotics

ORIGINAL ARTICLE

Bio-Inspired Transparent Soft Jellyfish Robot

Yuzhe Wang,[1,2] Pengpeng Zhang,[2] Hui Huang,[1] and Jian Zhu[3,4]

Abstract

Jellyfish are among the widely distributed nature creatures that can effectively control the fluidic flow around their transparent soft body, thus achieving movements in the water and camouflage in the surrounding environments. Till now, it remains a challenge to replicate both transparent appearance and functionalities of nature jellyfish in synthetic systems due to the lack of transparent actuators. In this work, a fully transparent soft jellyfish robot is developed to possess both transparency and bio-inspired omni motions in water. This robot is driven by transparent dielectric elastomer actuators (DEAs) using hybrid silver nanowire networks and conductive polymer poly(3,4-ethylenedioxythiophene):poly(styrenesulfonate)/waterborne polyurethane as compliant electrodes. The electrode exhibits large stretchability, low stiffness, high transmittance, and excellent conductivity at large strains. Consequently, the highly transparent DEA based on this hybrid electrode, with Very-High-Bond membranes as dielectric layers and polydimethylsiloxane as top coating, can achieve a maximum area strain of 146% with only 3% hysteresis loss. Driven by this transparent DEA, the soft jellyfish robot can achieve vertical and horizontal movements in water, by mimicking the actual pulsating rhythm of an *Aurelia aurita*. The bio-inspired robot can serve multiple functions as an underwater soft robot. The hybrid electrodes and bio-inspired design approach are potentially useful in a variety of soft robots and flexible devices.

Keywords: soft robots, transparent electrodes, bio-inspiration, dielectric elastomers

Introduction

The ability to be transparent is a conspicuous advantage for nature creatures. The transparency allows them to camouflage in the surrounding environment, avoid predators and hide their movements. Robots with similar capabilities can be of great value for many applications, for instance, aiding surveillance and assisting research that involves observing animals in their natural habitats. In recent years, researchers have been working on artificial transparency to design bio-inspired transparent machines to mimic nature creatures.[1–6] Among the transparent natural creatures, *Aurelia aurita* (also called moon jelly), one of the most common jellyfish, can effectively control the fluidic flow around their body to achieve movement in the water, despite their simple body structure (Fig. 1A, B).[7] Jellyfish generally swim continuously upon the thrust generated by cyclic alterations in expanding and contracting the bell with different relative durations.[7]

The contraction is faster than the expansion, resulting in a larger proportion and a smaller dragging force, as illustrated in Figure 1B. In nature, many jellyfish are highly transparent

[1]Singapore Institute of Manufacturing Technology, Agency for Science, Technology and Research (A*STAR), Singapore.
[2]Department of Mechanical Engineering, National University of Singapore, Singapore.
[3]School of Science and Engineering, Chinese University of Hong Kong at Shenzhen, Shenzhen, China.
[4]Shenzhen Institute of Artificial Intelligence and Robotics for Society, Shenzhen, China.

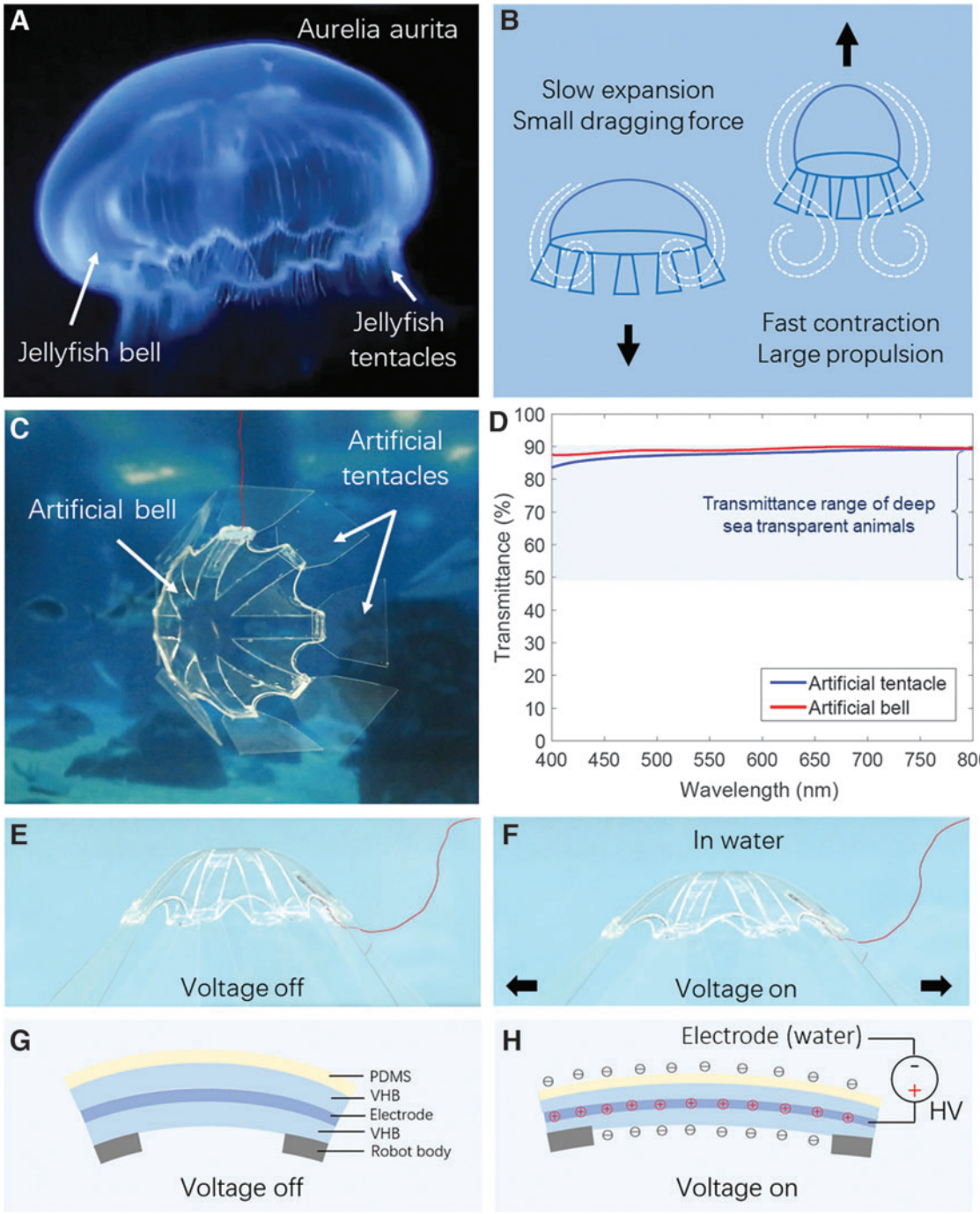

FIG. 1. Concept of the bio-inspired transparent soft jellyfish robot. **(A)** A picture of a natural jellyfish in the deep ocean. **(B)** Schematic of expansion and contraction states of a jellyfish. **(C)** A picture of the transparent soft jellyfish robot. **(D)** Transmittance over the visible spectrum for the soft jellyfish robot. **(E, F)** The voltage off and voltage on state of the jellyfish soft robot in water. The artificial bell opens when subject to voltage. **(G, H)** The actuation principle of the robot, and its voltage off/voltage on state.

and nearly invisible in water. Transparency is one of the effective ways to disguise themselves in the ocean and camouflage well against various backgrounds to avoid predators. Their transparent appearance and adaptability have inspired the design of underwater soft robots.[5,8–15] However, a jellyfish robot that can mimic both the exceptional functionality and appearance of natural jellyfish has yet to be developed, due to intrinsic limitations of actuators that prohibit their integration in a flexible, lightweight, and transparent manner. These properties are extremely desirable for jellyfish-inspired soft robots.

Previous attempts have been made to develop soft robots to achieve jellyfish-like locomotion using stimuli-responsive actuators, including pneumatic structures,[16–18] shape memory alloys,[10,13,19] ionic polymer metal composites,[9,20,21] magnetic composite elastomer,[8,22] twisted coiled polymer actuators,[23]

and dielectric elastomer actuators (DEAs).[5,12,24–26] These actuators have shown promising geometrical adaptability and high compliance compared to electrical motors, and DEAs stand out among them due to interesting attributes such as large voltage-induced deformation, high energy density, fast response, low weight, and quiet operation.[27–29] Recently, several jellyfish soft robots have been developed using DEAs,[24,25] and these soft robots used carbon-based electrodes, which are the most common electrode material for DEAs.[30] Although carbon-based DEAs allowed the robots to achieve jellyfish-like morphology and movements, they could not accurately mimic the actual transparent appearance of jellyfish, since carbon-based electrodes are black and opaque.

Transparency of soft jellyfish robots enables passive camouflage, which eliminates the need for foreknowledge and adaptation to the background and surrounding environment, as commonly required in active camouflage strategies.[31,32] Previous works also have demonstrated the patterning of ionic hydrogels[33] and single-walled carbon nanotube[34,35] to serve as optically transparent electrodes. However, ionic hydrogel-based actuators/robots are usually thick, which leads to large refraction and scattering effects, and the transmittance of single-walled carbon nanotube-based soft actuators are usually low. Thus, the key challenge is to create a fully transparent soft jellyfish robot with transparent materials and smart actuation methods that can achieve muscle-like large deformation and fast contraction.

Silver nanowires (AgNWs) have attracted many focuses recently in fabricating electronic devices due to their notable electrical conductivity.[36] AgNW-based electrodes have been utilized in numerous optoelectronic devices such as organic photovoltaics and organic light-emitting diodes. However, only a few works have been reported using AgNWs as compliant electrodes for DEAs, although AgNW networks are mechanically flexible and highly conductive.[37,38] This is because AgNW networks exhibit fast increase in sheet resistance upon stretching and the interlinked cross joint may break when subjected to large strains during actuation.

In this article, we present a highly transparent DEA using hybrid AgNW networks and conductive polymer poly(3,4-ethylenedioxythiophene):poly(styrenesulfonate)/water-born polyurethane (PEDOT:PSS/WPU) as compliant electrodes, with Very-High-Bond (VHB) membranes as dielectric layers and polydimethylsiloxane (PDMS) as the top coating. The PEDOT:PSS/WPU layer binds AgNW network firmly to the VHB membrane, thus lowering the sheet resistance and enabling the hybrid electrodes to remain highly conductive when DEAs exhibit large voltage-induced deformations.

The DEA has a highly transparent multilayer structure, and the electrodes possess low sheet resistance when subject to large strains. The DEA can achieve a maximum area strain of 146% with only 3% hysteresis loss, which enables muscle-like large expansion and fast contraction. Inspired by the structure and moving mechanism of *A. aurita*, a fully transparent soft jellyfish robot driven by DEAs with AgNW/PEDOT:PSS hybrid electrodes is developed (Fig. 1C). The jellyfish soft robot can mimic both appearance and functionalities of natural jellyfish to camouflage in water during its locomotion by using bio-inspired stimuli similar to the actual pulsating rhythm of an *A. aurita*. The bio-inspired design and biomimetic moving mechanism of this transparent soft jellyfish robot provide its feasibility to serve multiple functions as an underwater soft robot.

Materials and Methods

Materials of the DEA

PEDOT:PSS aqueous solution (Clevios PH 1000 Lot 2015P0052) is purchased from Heraeus. It has a concentration of 1.3 wt%, and the PSS-to-PEDOT weight ratio is 2.5. WPU (WPU-3-501D) is supplied by the Taiwan PU Corporation, which is a polyester-based nonionic polyurethane water dispersion with a concentration of 40 wt%. Ethylene glycol (EG) is purchased from J.T. Baker. Polyether-modified PDMS (BYK-333) is obtained from BYK Additives & Instruments. PDMS (Sylgard 184) is supplied by the Dow Chemical Company. All the chemicals are used as received without further purification.

Fabrication of the hybrid transparent electrode

PEDOT:PSS aqueous solution is added with 5 vol% EG, which is then mixed with 10 wt% WPU aqueous solution. The loading of PEDOT:PSS in the PEDOT:PSS/WPU blends is 5 wt%. Then, 0.1 wt% BYK-333 is added into the WPU/PEDOT:PSS aqueous solution. The addictive can improve the wettability of the PEDOT:PSS/WPU water dispersion on the surface of VHB film and reduce the surface tension of the coatings. The solution is used for the preparation of the PEDOT:PSS/WPU thin layer.

Silver nitrate, EG, iron chloride, and polyvinylpyrrolidone ($Mw = 55{,}000$) are used to synthesize AgNWs. AgNWs are grown at 140°C in an automated synthesis system using the modified polyol process.[39,40] They are washed thrice in isopropanol (IPA) and then dispersed in IPA with a concentration of 1 wt% for coating. The synthesized AgNWs have an average diameter of 60 nm and an average length of 70 μm. Bar coating is used to deposit AgNWs.

The protective covers for VHB rolls (3M) are used as the substrate due to their smooth surface and nonstick properties to VHB and PDMS. The substrate is cleaned thoroughly by IPA to improve the dispersion of AgNW solution during the coating process. The AgNWs with increasing loading density of 0.5, 1.0, 1.5, and 2.0 g/m^2 are coated on the substrates by the film applicator, and the four samples are labeled as PT-Ag0.5, PT-Ag1.0, PT-Ag1.5, and PT-Ag2.0, respectively.

Fabrication of the PDMS top coating layer

PDMS is one kind of silicone elastomer that has good biocompatibility, high stretchability, excellent optical properties, and ease of molding. PDMS mixture is prepared by mixing pre-polymer (base) and crosslinker (curing agent) components with a weight ratio of 15:1. The mixture is thoroughly mixed and degassed in a vacuum chamber for 20 min. The degassed PDMS mixture is coated on top of the electrodes by a wired K-Bar No.0 rod (RK Print Coat Instruments Ltd., United Kingdom). Finally, the wet film is cured at 70°C for 5 h.

Performance characterization

The actuators and the jellyfish robot are connected to a voltage amplifier (TREK 20/40A). The videos are recorded using a DSLR camera (Sony 6D). Sheet resistances of the electrodes are measured by an inline Noncontact Eddy Current Sheet Resistance Meter (Delcom Instruments, Inc.).

Results and Discussion

This bio-inspired soft jellyfish robot is composed of an artificial bell with transparent DEAs and eight artificial tentacles made of 400 μm-thick polyethylene terephthalate (PET) sheets. The entire robot is highly transparent since all the VHB membranes, electrodes, and PET sheets are transparent (Fig. 1C). The average transmittance of the artificial bell and artificial tentacles over the visible light spectrum measured in the air as the medium are 89% and 87%, respectively (Fig. 1D), which are within the transmittance range of deep-sea transparent animals of (50–90%).[41]

Although the indexes of the robot membrane and water do not differ a lot and the robot membranes are very thin, the robot is still visible in water when observed through certain angles due to light reflections since all the materials used to fabricate the robot have very smooth surfaces. In addition, the thickness differences between ''VHB membrane-only region'' and ''PET+VHB membrane region'' may further increase the visibility of the robot in water. Several measures can be considered to reduce visibility of the robot in water, such as using thinner frames and smoothen the interface between PET and VHB membrane to avoid sudden change in thickness.

The artificial bell consists of one layer of hybrid AgNW/PEDOT:PSS transparent electrode encapsulated between two layers of VHB membrane, and a thin layer of PDMS top coating (Fig. 1G). The electrodes are well sealed and will not contact with water during operation. When the robot is in the water, the surrounding fluid is served as the ground electrode (Fig. 1H), eliminating the need to fabricate and encapsulate the other electrode layer, which would further stiffen and thicken the DEAs. Thin copper wires with insulation layer are used to connect the jellyfish robot by drop coating PEDOT:PSS/WPU-AgNW ink on the joint. When connected to voltage, the actuators are subjected to the voltage-induced Maxwell stress, resulting in a decrease in thickness and an expansion in area.

When subjected to AC signals, this process repeats and causes the entire robot body to pulsate like a natural jellyfish (Fig. 1E, F). Figure 2 illustrates the fabrication process of this robot. Two dielectric elastomer membranes (VHB4910; 3M) with biaxial prestretches of 3.5 times are attached to a circular flexible PET frame with eight identical blanks circularly distributed about its geometrical center. Before attaching VHB to PET, the surface of PET is cleaned thoroughly by using IPA and acetone to ensure strong adhesion between VHB and PET. The PET frame is a circle with a diameter of 110 mm and a thickness of 0.5 mm. Each blank is a circle sector with a radius of 42 mm and a central angle of 45° as shown in Figure 2.

The AgNW suspension in isopropanol is coated on the protective cover for VHB rolls using a bar-type film applicator and then transferred to the prestretched VHB membrane after resting at room temperature for 10 min. Then, PEDOT:PSS/WPU dispersion is spin-coated on AgNW electrode area followed by curing at 60°C for 60 min. The PEDOT:PSS/WPU coating binds AgNW network firmly to the VHB membrane, forming the hybrid electrode. Subsequently, another two VHB membranes with biaxial prestretches of 3.5 times are attached on top of the electrode layer. Then, 4 μm-thick degassed PDMS mixture (Sylgard 184; The Dow Chemical Company; pre-polymer to cross-linker weight ratio 15:1) is coated on the actuator by a wired bar (K-Bar No. 0) followed by curing at 70°C for 5 h (Fig. 2).

The mechanical constraint for prestretching VHB membranes is then released; thus, the structure deforms into a 3D bell-like shape, characterized by the dielectric elastomer minimum energy structure (DEMES), as illustrated in Figure 2. Finally, eight artificial tentacles made of 400 μm-thick PET are attached to the robot body. The artificial tentacles can increase the propulsion and achieve more effective movement in the water. The as-fabricated jellyfish robot is only 9.1 g in weight, with a height of 71 mm and a maximum diameter of 104 mm at its reference state.

Figure 3A shows the stress-strain relation of the hybrid AgNW/PEDOT:PSS transparent electrodes with different AgNW loadings, and the electrodes impose minor constraints on the membranes. The hybrid electrodes are highly stretchable and can be stretched up to three times their initial length. Figure 3C shows the variation of sheet resistances of

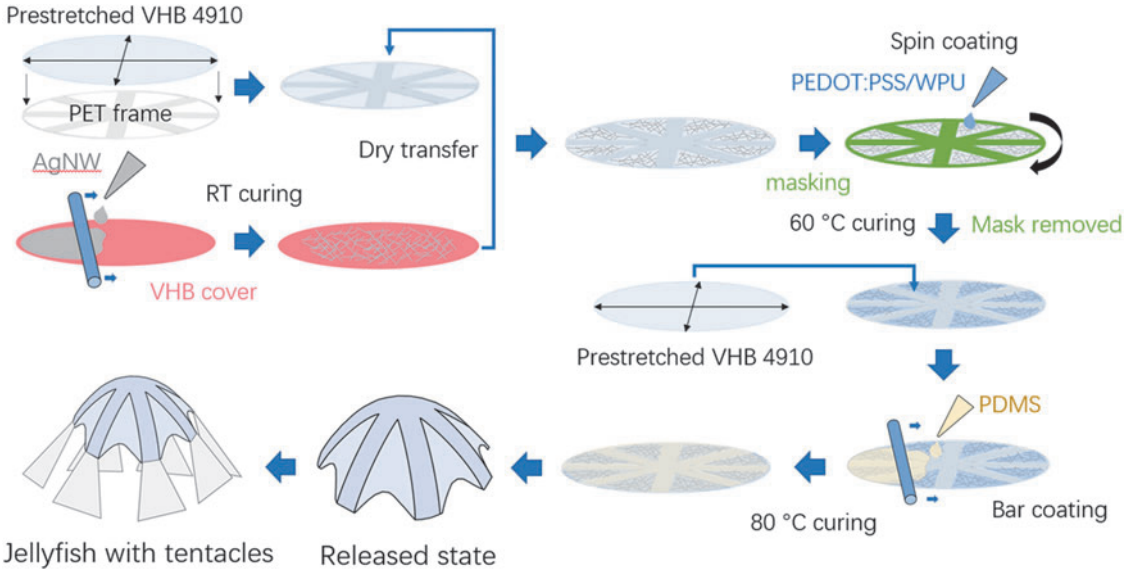

FIG. 2. Fabrication processes of the multilayer structure of the transparent jellyfish soft robot.

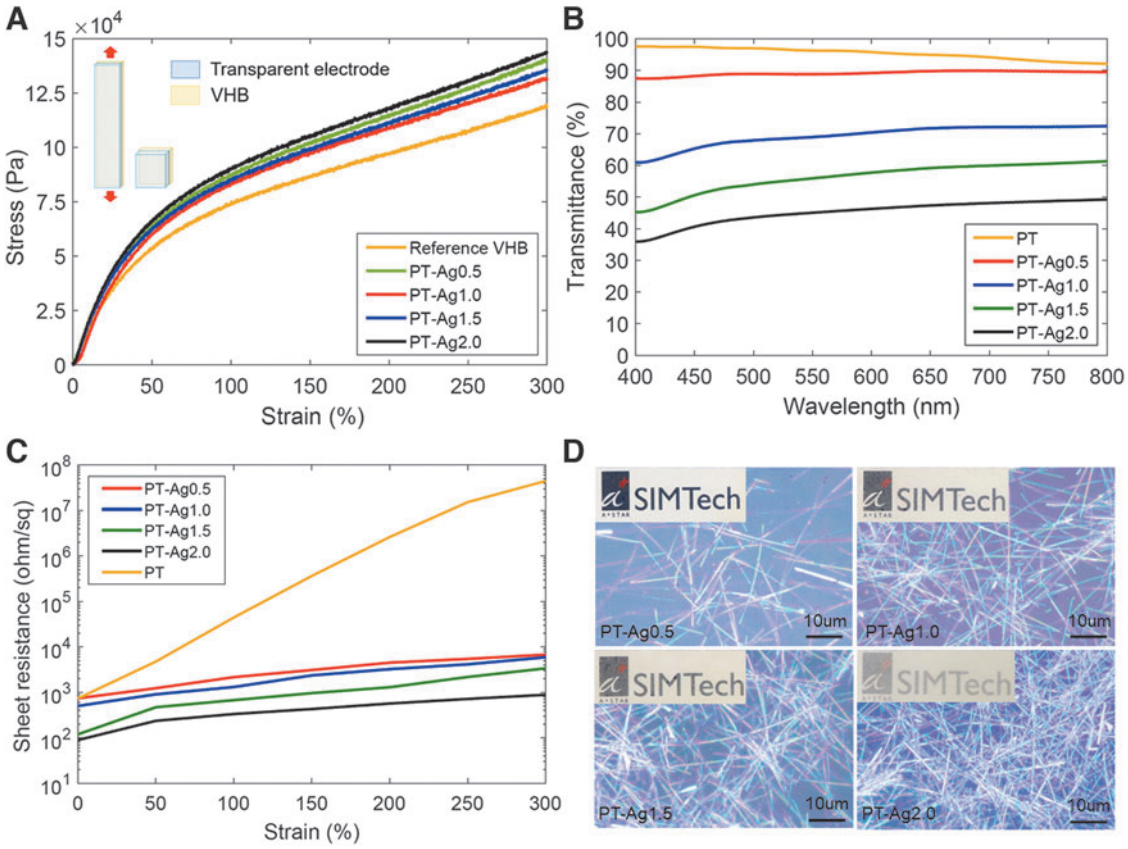

FIG. 3. Characterization of the four hybrid AgNW/PEDOT:PSS transparent electrode samples with increasing AgNW loadings of 0.5 g/m^2 (PT-Ag0.5), 1.0 g/m^2 (PT-Ag1.0), 1.5 g/m^2 (PT-Ag1.5), and 2.0 g/m^2 (PT-Ag2.0). **(A)** Strain-stress relation for the AgNW/PEDOT:PSS electrode materials on a VHB membrane. **(B)** Transmittances of the transparent electrodes on a pre-stretched VHB membrane. **(C)** Variations of the sheet resistance change of the electrodes on the VHB membrane when subject to tensile strains. The sheet resistances are compared to PEDOT:PSS/WPU electrodes (*yellow line*). **(D)** Images of AgNW networks with PEDOT:PSS/WPU blend under the microscope and their transparency on a SIMTech logo. AgNW, silver nanowire; PEDOT:PSS/WPU, poly(3,4-ethylenedioxythiophene):poly(styrenesulfonate)/waterborne polyurethane; VHB, Very-High-Bond.

the electrodes on a VHB membrane as a function of linear strains. The sheet resistances of the hybrid electrodes are much less sensitive to the strains compared to the PEDOT:PSS/WPU transparent electrodes, and higher AgNW loadings result in even lower sheet resistances. For the hybrid electrodes with 0.5 g/m^2 AgNW loading (PT-Ag0.5), the sheet resistance becomes nine times its initial resistance at the strain of 300%.

For the electrode with 2.0 g/m^2 AgNW loading (PT-Ag2.0), the resistance can remain below 1000 Ω/sq at the strain of 300%. As a result, the hybrid electrodes can remain highly conductive when DEAs exhibit large voltage-induced deformations. Transparency of the electrode is one of the key properties in mimicking the transparent feature of natural jellyfish. Figure 3D shows that the electrode is highly transparent at low AgNW loadings, and the transparency decreases with increasing AgNW loadings due to denser nanowire networks. For example, PT-Ag0.5 exhibits an average transmittance of 90% in the whole visible light range, and it is only 5% lower compared with PEDOT:PSS/WPU transparent electrodes (Fig. 3B).[6] Consequently, PT-Ag0.5 electrode is preferred for fabricating transparent DEAs, due to its large stretchability, high transmittance, and low sheet resistance sensitivity to strains.

It is significant for a DEA to achieve large voltage-induced deformation, to mimic the muscle-like contraction and expansion of a bio-inspired soft jellyfish robot. Figure 4A illustrates the schematics of a common circular DEA used to investigate the electromechanical behavior of DEAs. Figure 4B shows the actuation performance of a transparent DEA on a background of SIMTech logos. The center part is coated with the electrodes and functions as a DEA.

When subject to voltage, the center active part expands its area, and the actuation strain is systematically evaluated by applying a ramp voltage at a constant ramping rate of 100 V/s from 0 kV until the actuator fails. The experiments demonstrate that the DEA with PT-Ag0.5 can achieve a large voltage-induced area strain of 146% at 12 kV (Fig. 4C). The PDMS top coating plays a significant role in reducing hysteresis losses during cyclic actuation. Figure 4D and E compare the area strains and hysteresis losses for DEAs made of various materials. As we can see from Figure 4D, the DEA with conventional carbon grease electrode exhibits the largest area strain, but a significant hysteresis loss. PDMS layers are less viscoelastic, and they can reduce the hysteresis loss result from highly

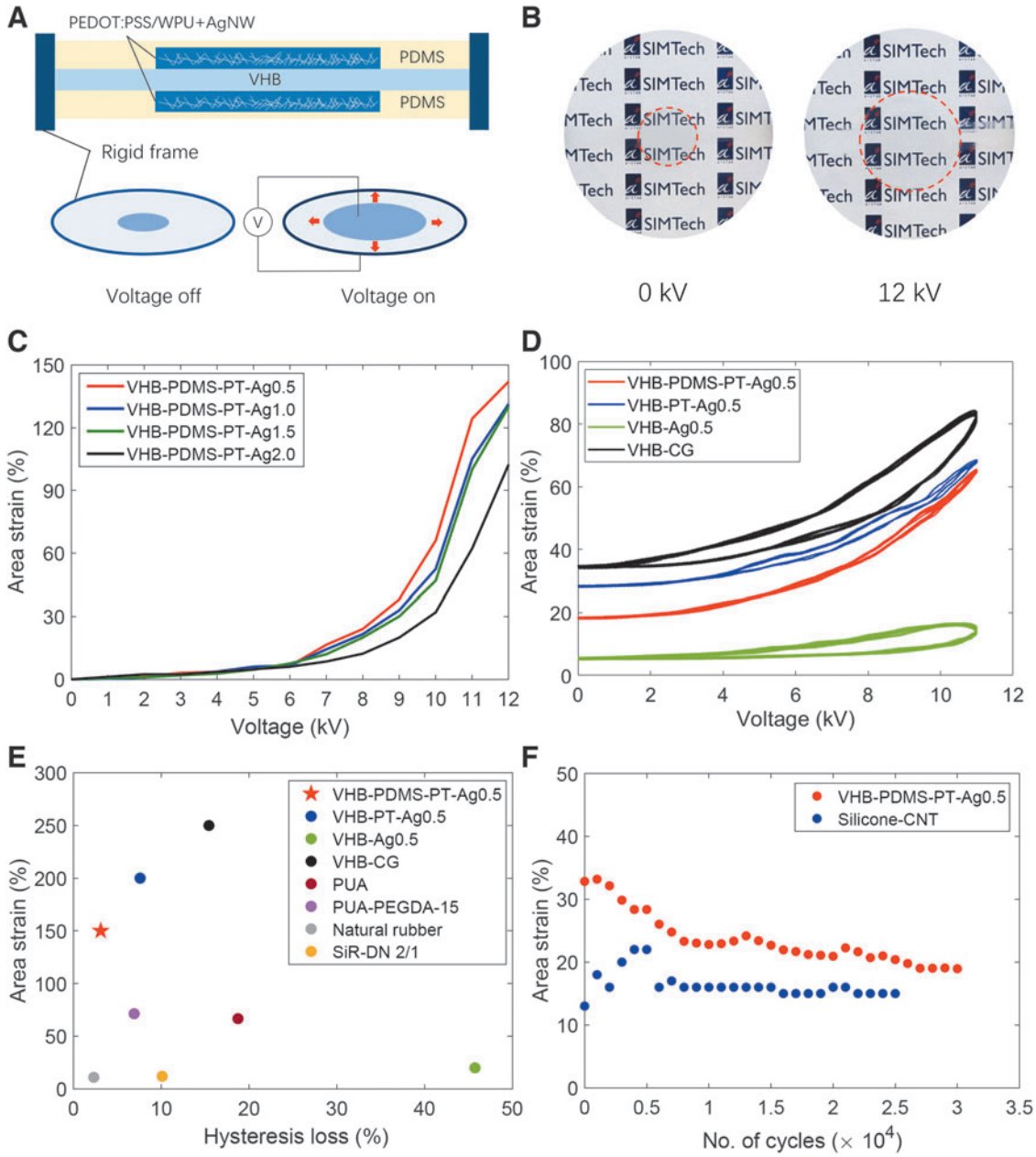

FIG. 4. Performance of the transparent DEAs. **(A)** The multilayer structure of the transparent DEA, and the actuation principle of a DEA. **(B)** Transparent DEA using AgNW/PEDOT:PSS electrodes at voltage off and on states with an area strain of 146% (The *dashed circle lines* are used for easy visualization of the area expansion since the electrode areas were transparent and hard to identify). **(C)** Area strain as a function of voltage for actuators (VHB-PDMS-PEDOT:PSS/WPU-AgNW structure) using increasing AgNW loadings from 0.5 to 2.0 g/m^2). **(D)** Area strain as a function of voltage under cyclic AC voltage, for AgNW-embedded PEDOT:PSS/WPU with PDMS coating (VHB-PDMS-PT-Ag0.5), AgNW-embedded PEDOT:PSS/WPU (VHB-PT-Ag0.5), AgNW electrode only (VHB-Ag0.5), and carbon grease electrode (VHB-CG). **(E)** Maximum area strains and hysteresis losses compare to DEAs in the literature, such as PUA, PUA copolymerized with polyethylene glycol diacrylate, natural rubber, and dual-crosslinking network of Silicon rubber (SiR-DN 2/1). **(F)** Area strain as a function of the number of cycles performed under 1 Hz 10 kV AC voltage and compare to silicone-carbon nanotube-based DEAs. DEA, dielectric elastomer actuator; PDMS, polydimethylsiloxane; PUA, polyurethane acrylate; SiR-DN, silicon rubber.

viscoelastic VHB to 3%, while the actuator can still achieve a maximum area strain of 146%.

The DEA based on VHB-PDMS-PEDOT:PSS/WPU-AgNW structure exhibits the lowest hysteresis loss than those DEAs made of other dielectric materials and electrodes in the literature (Fig. 4E), such as polyurethane acrylate, natural rubber, and dual-crosslinking network of silicon rubber.[42–45] This characteristic is significant for mimicking the fast contraction of natural jellyfish. In addition, the PDMS layer enhances the bonding between the electrode and the dielectric

elastomer, minimizing the possibility of slipping or detachment from the dielectric elastomer, and avoiding mechanical break of electrodes. Thus, the developed DEA exhibits excellent durability and can be actuated by a 2 Hz 10 kV AC voltage at large operational area strains for at least 30,000 cycles (Fig. 4F). Actually, the actuator can still be actuated after the 30,000 cycles' test. Both the operational area strain and the number of cycles performed are greater than the DEA made of silicone and carbon nanotube.[45]

The decrease in actuation strains may be due to the relaxation of VHB membranes and the increase in sheet resistance during cyclic operation. The enhanced performance is attributed to the synergy of AgNWs, PEDOT:PSS/WPU, VHB, and PDMS multiple layers. Longer product life spans can contribute to eco-efficiency and sufficiency, thus minimizing excessive maintenance or repair. Consequently, considering the voltage-induced deformation, transmittance, hysteresis loss, and lifetime, the hybrid AgNW/PEDOT:PSS-based DEAs can be an excellent option for the bio-inspired transparent soft jellyfish robot.

The transparent soft jellyfish robot, made of transparent DEAs based on hybrid AgNW/PEDOT:PSS electrodes, can achieve effective motions in the water. Figure 5A and Supplementary Movie S1 (Supplementary Materials) illustrate the vertical motion when DEAs are subjected to a 2 Hz 5 kV voltage. The expansion and contraction behaviors of the artificial bell are similar to a natural jellyfish. As shown in Figure 5B, a natural jellyfish can perform rowing motion by pulsating its bell.[7,46] In each cycle, the bell expands slowly (in 0.4 s), followed by a fast contraction (in 0.25 s) to reduce

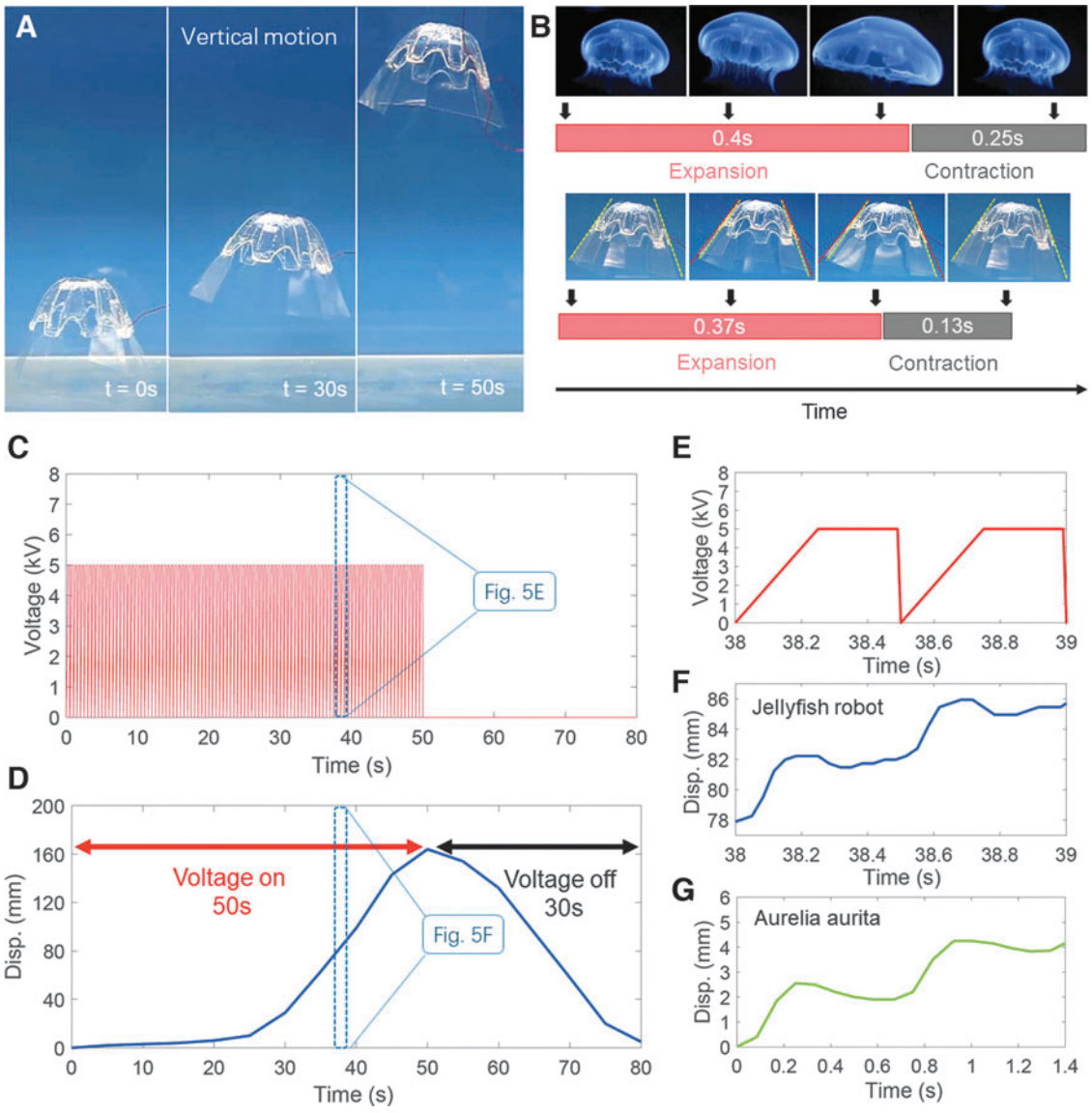

FIG. 5. Vertical movements of the transparent jellyfish robot in water. **(A)** The transparent soft jellyfish robot moves up in the water when subject to defined voltage signals. **(B)** The jellyfish robot expands its bell slowly and contracts fast, mimicking a natural jellyfish swimming in water. **(C)** The defined voltage signals applied to the robot for 50 s. **(D)** Vertical displacement as a function of time when the robot is moving in water for 80 s. **(E)** Enlarged view of the bio-inspired voltage applied on the jellyfish robot from 38 to 39 s. **(F)** The enlarged view of the vertical displacement as a function of time when the robot moves in water from 38 to 39 s. **(G)** Vertical movement trajectory of a natural jellyfish (*Aurelia aurita*).

the volume enclosed by the bell and generate the expulsion of fluid through the opening.[7] It should be noted that the tentacles of natural jellyfish are used for predation and self-defense, while the artificial tentacles on the jellyfish robot can significantly increase the propulsion and contribute to effective movements in the water.

The soft jellyfish robot follows a similar pulsating rhythm as natural jellyfish by applying a defined voltage signal as shown in Figure 5E. This signal is designed to mimic the actual pulsating rhythm of an *A. aurita*. A ramp voltage from 0 to 5 kV with a ramping rate of 20 kV/s is first applied for 0.25 s, and a constant voltage of 5 kV is maintained for another 0.25 s, followed by an immediate decrease to 0 kV at $t = 0.5$ s. The entire cycle takes 0.5 s, and such input signal is repeated one after another at a frequency of 2 Hz. When the robot is subjected to this voltage signal, the artificial bell expands gradually in 0.37 s and then contracts fast in 0.13 s.

This pulsating rhythm results in a large proportion and a small dragging force. As shown in Figure 5F, when the artificial bell is expanding, the robot has a small downward moving trend. This is due to both the dragging force and gravity of the robot body. When the voltage decreases from

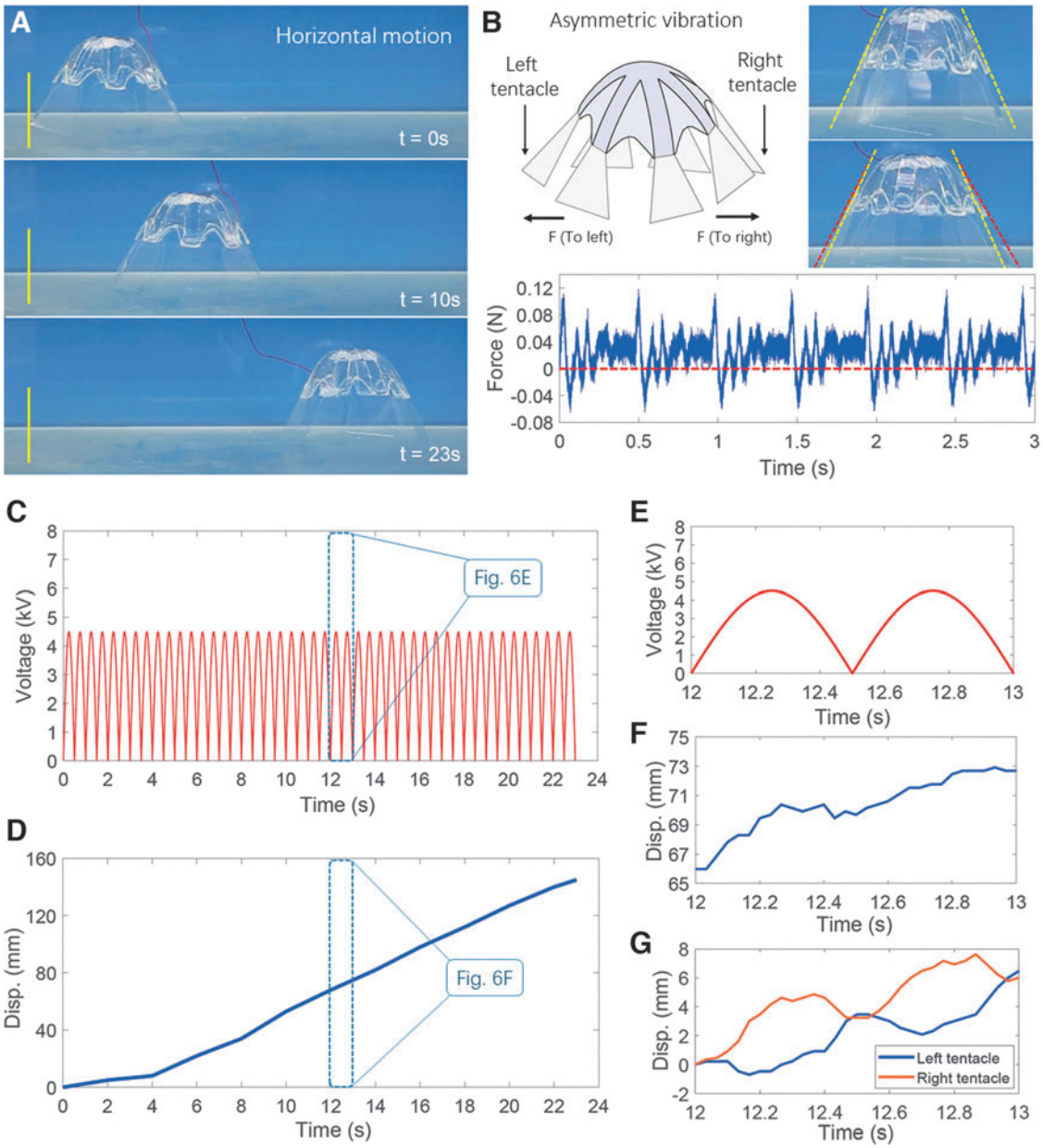

FIG. 6. Horizontal movements of the transparent jellyfish robot in water. **(A)** The transparent soft jellyfish robot moves horizontally in the water when subject to sine voltage signals. **(B)** The jellyfish robot vibrates asymmetrically when subject to sine voltage signals of 4.5 kV and 2 Hz, resulting in asymmetrical forces. **(C)** The voltage signals applied to the robot for 23 s. **(D)** Horizontal displacement as a function of time of the robot moving in water for 23 s. **(E)** Enlarged view of the voltage applied to the jellyfish robot from 12 to 13 s. **(F)** The enlarged view of the horizontal displacement as a function of time when the robot is moving in water from 12 to 13 s. **(G)** Displacement as a function of time for the *right* (*orange curve*) and *left* (*blue curve*) tentacles when the robot is moving horizontally in the water.

5 to 0 kV immediately, the robot moves up fast due to the sudden contraction of the artificial bell (Supplementary Movie S2). It should be noted that there is a delay of ~ 0.15 s between the applied voltage and robot displacements. This may be because the robot must move against the resistance of the water. The vertical moving trajectory of the robot (Fig. 5F) is very close to the one of an *A. aurita*,[7] as shown in Figure 5G.

The experimental results show that this jellyfish robot is capable of mimicking the vertical movements of a natural jellyfish effectively, in terms of both appearance and functionality. When the input voltage signal is applied for 50 s and turned off for 30 s (Fig. 5C), the robot can achieve a complete up-and-down movement with 160 mm upward floating displacement in 50 s at an average speed of 5.4 mm/s (Fig. 5D), followed by a fall in the water with an average speed of 5.3 mm/s, and the robot reaches the ground at $t = 80$ s. It should be noted that lower voltage could be the cause of the slower movement of the robot. However, higher voltage may cause electromechanical breakdown and shorten the lifetime of the robot. We keep a lower voltage for safer operation.

Natural jellyfish depends mainly upon ocean currents for horizontal movements. However, our soft jellyfish robot can move horizontally by the asymmetric vibration of its artificial bell. As shown in Figure 6A and Supplementary Movie S3 (Supplementary Materials), the asymmetric vibration of the artificial bell is caused by the asymmetrical mode of the structure when subjected to a specific actuation frequency.

It is an inherent characteristic for DEMES to respond with different vibration modes when the DEAs are subjected to voltages of different waveforms and frequencies. In the case of sine voltage signals of 4.5 kV and 2 Hz, the asymmetric vibration mode is dominant, indicated by different displacements of the left and right tentacles. When the robot body and tentacles on the right side vibrate greater than that on the left side (top right of Fig. 6B), the force to the right is thus greater than the force to the left (bottom of Fig. 6B), causing the robot moving to the right. Force values above the red dashed line at the bottom of Figure 6B indicate forces to the right (peak value 0.12 N), and the values below the red dashed line indicate forces to the left (peak value 0.06 N).

In the experiments, the sinusoid voltage is applied for 23 s (Fig. 6C), and the jellyfish robot moves 145 mm horizontally at an average speed of 6.3 mm/s (Fig. 6D). Figure 6E–G show the applied voltage, the horizontal displacements of the robot, and the displacements of tentacles on both sides for two complete cycles, respectively. It can be noticed from Figure 6G that the tentacles on the right side have larger displacements than those on the left side throughout the entire cycle, which is consistent with the video frames shown in Figure 6B for asymmetric vibration. In this work, we mainly focus on the horizontal movement on the tank bottom. Strategies which can enable the robot to swim horizontally away from the tank bottom, such as multi-degree-of-freedom shape morphing, deserve further study.

Conclusion

This article presents an *A. aurita*-inspired transparent soft jellyfish robot based on highly transparent DEAs using AgNW/PEDOT:PSS hybrid electrodes with a multilayer structure. Although transparent DEAs have been developed so far to drive soft robots, the performance of the actuators is constrained by strong viscoelastic effects, short lifetime, and fast increasing sheet resistance upon stretching. Besides, few efforts have been previously made to resemble the appearance of natural jellyfish to achieve passive camouflage. In this work, the mechanical, electrical, and optical properties of the DEA are enhanced by the hybrid electrodes, and the DEA can achieve a large voltage-induced area strain of 146% and a high transmittance of 89%. The PDMS top coating layer protects the actuator and reduces hysteresis loss during cyclic actuation.

The jellyfish robot based on the hybrid electrodes is thin and highly transparent, so it can mimic both appearance and functionalities of natural jellyfish to camouflage in water during its vertical and horizontal movements. The bio-inspired design and biomimetic moving mechanism of this transparent soft jellyfish robot provide the feasibility to serve multiple functions as an underwater soft robot. The improved durability of the electrodes and actuators can ensure the robot has a longer lifetime and operates in harsh environments. Biologists can take advantage of this robot to study sea animal behaviors such as the predator's actions underwater without any interruption to them. Other potential applications are underwater detection and security surveillance. For future developments, the self-sensing capability of DEAs may provide the feasibility for self-monitoring, water depth feedback, and reinforcement learning-based control, which may significantly enrich the functionalities of the transparent soft jellyfish robot.

Data and Materials Availability

Data are available from the authors upon request.

Authors' Contributions

Y.W., H.H., and J.Z. conceived the concept and wrote the article. Y.W. and P.Z. carried out the experiments. H.H. guided material fabrication. H.H. and J.Z. directed the project. All authors analyzed and interpreted the data.

Author Disclosure Statement

No competing financial interests exist.

Funding Information

Y.W. acknowledges the support from A*STAR, Singapore (iGrant No. C211518007). J.Z. acknowledges the support from the Start-up Funding at the Chinese University of Hong Kong, Shenzhen (UDF01001987), and Shenzhen Institute of Artificial Intelligence and Robotics for Society (AC01202101113).

Supplementary Material

Supplementary Materials
Supplementary Movie S1
Supplementary Movie S2
Supplementary Movie S3

References

1. Lee H, Kim H, Ha I, et al. Directional shape morphing transparent walking soft robot. Soft Robot 2019;6(6):760–767; doi: 10.1089/soro.2018.0164

2. Li T, Li G, Liang Y, et al. Fast-moving soft electronic fish. Sci Adv 2017;3(4):e1602045; doi: 10.1126/sciadv.160204
3. Keplinger C, Sun J-Y, Foo CC, et al. Stretchable, transparent, ionic conductors. Science 2013;341(6149):984–987; doi: 10.1126/science.1240228
4. Yuk H, Lin S, Ma C, et al. Hydraulic hydrogel actuators and robots optically and sonically camouflaged in water. Nat Commun 2017;8:14230; doi: 10.1038/ncomms14230
5. Christianson C, Goldberg NN, Deheyn DD, et al. Translucent soft robots driven by frameless fluid electrode dielectric elastomer actuators. Sci Robot 2018;3(17):eaat1893; doi: 10.1126/scirobotics.aat1893
6. Li P, Wang Y, Gupta U, et al. Transparent soft robots for effective camouflage. Adv Funct Mater 2019;29(37): 19019081901908; doi: 10.1002/adfm.201901908
7. Costello, JH, Colin SP. Morphology, fluid motion and predation by the scyphomedusa *Aurelia aurita*. Adv Mar Biol 1994;(121):327–334; doi: 10.1007/BF00346741
8. Ren Z, Hu W, Dong X, et al. Multi-functional soft-bodied jellyfish-like swimming. Nat Commun 2019;10(1):2703; doi: 10.1038/s41467-019-10549-7
9. Yeom S W, Oh IK. A biomimetic jellyfish robot based on ionic polymer metal composite actuators. Smart Mater Struct 2009;18(8):085002; doi: 10.1088/0964-1726/18/8/085002
10. Tadesse Y, Villanueva A, Haines C, et al. Hydrogen-fuel-powered bell segments of biomimetic jellyfish. Smart Mater Struct 2012;21(4):045013; doi: 10.1088/0964-1726/21/4/045013
11. Yang Y, Ye X, Guo S. A new type of jellyfish-like microrobot. In: 2007 IEEE International Conference on Integration Technology. IEEE: Shenzhen, China; 2007.
12. Christianson C, Bayag C, Li G, et al. Jellyfish-inspired soft robot driven by fluid electrode dielectric organic robotic actuators. Front Robot AI 2019;6(November):1–11; doi: 10.3389/frobt.2019.00126
13. Villanueva A, Smith C, Priya S. A biomimetic robotic jellyfish (robojelly) actuated by shape memory alloy composite actuators. Bioinspir Biomim 2011;6(3):036004; doi: 10.1088/1748-3182/6/3/036004
14. Zhou Y, Jin H, Liu C, et al. A novel biomimetic jellyfish robot based on a soft and smart modular structure (SMS). In: 2016 IEEE International Conference on Robotics and Biomimetics (ROBIO). IEEE: Qingdao, China; 2016.
15. Nawroth JC, Lee H, Feinberg AW, et al. A tissue-engineered jellyfish with biomimetic propulsion. Nat Biotechnol 2012;30(8):792–797; doi: 10.1038/nbt.2269
16. Frame J, Lopez N, Curet O, et al. Thrust force characterization of free-swimming soft robotic jellyfish. Bioinspir Biomim 2018;13(6):064001; doi: 10.1088/1748-3190/aadcb3
17. Chi Y, Tang Y, Liu H, et al. Leveraging monostable and bistable pre-curved bilayer actuators for high-performance multitask soft robots. Adv Mater Technol 2020;5(9): 2000370; doi: 10.1002/admt.202000370
18. Joshi A, Kulkarni A, Tadesse Y. FludoJelly: Experimental study on jellyfish-like soft robot enabled by soft pneumatic composite (SPC). Robotics 2019;8(3):56; doi: 10.3390/robotics8030056
19. Cruz Ulloa C, Terrile S, Barrientos A. Soft underwater robot actuated by shape-memory alloys ''jellyrobcib'' for path tracking through fuzzy visual control. Appl Sci 2020; 10(20):7160; doi: 10.3390/app10207160
20. Najem J, Sarles SA, Akle B, et al. Biomimetic jellyfish-inspired underwater vehicle actuated by ionic polymer metal composite actuators. Smart Mater Struct 2012;21(9):94026; doi: 10.1088/0964-1726/21/9/094026
21. Najem J, Akle B, Sarles SA, et al. Design and development of a biomimetic jellyfish robot that features ionic polymer metal composites actuators. In: ASME 2011 Conference on Smart Materials, Adaptive Structures and Intelligent Systems. American Society of Mechanical Engineers. Scottsdale, Arizona, USA. 2011;691–698; doi: 10.1115/SMASIS2011-5105
22. Ren Z, Wang T, Hu W, et al. A Magnetically-Actuated Untethered Jellyfish-Inspired Soft Milliswimmer. In: Robotics: Science and Systems 2019: Freiburg im Breisgau, Germany, June 22–26.
23. Hamidi A, Almubarak Y, Rupawat YM, et al. Poly-saora robotic jellyfish: Swimming underwater by twisted and coiled polymer actuators. Smart Mater Struct 2020;29(4): 45039; doi: 10.1088/1361-665X/ab7738
24. Godaba H, Li J, Wang Y, et al. A soft jellyfish robot driven by a dielectric elastomer actuator. IEEE Robot Autom Lett 2016;1(2):624–631; doi: 10.1109/LRA.2016.2522498
25. Shintake J, Shea H, Floreano D. Biomimetic underwater robots based on dielectric elastomer actuators. In: 2016 IEEE/RSJ International Conference on Intelligent Robots and Systems (IROS). IEEE: Daejeon, Korea (South); 2016: 4957–4962; doi: 10.1109/IROS.2016.7759728
26. Cheng T, Li G, Liang Y, et al. Untethered soft robotic jellyfish. Smart Mater Struct 2018;28(1):15019; doi: 10.1088/1361-665X/aaed4f
27. Carpi F, Bauer S, De Rossi D. Stretching dielectric elastomer performance. Science 2010;330(6012):1759–1761; doi: 10.1126/science.1194773
28. Ashley S. Artificial muscles. Sci Am 2008;18(1):64–71; doi: 10.1038/scientificamerican1003-52
29. Pelrine RE, Kornbluh RD, Pei Q, et al. High-speed electrically actuated elastomers with strain greater than 100%. Science 2000;287(5454):836–839; doi: 10.1126/science.287.5454.836
30. Rosset S, Shea HR. Flexible and stretchable electrodes for dielectric elastomer actuators. Appl Phys A Mater Sci Process 2013;110(2):281–307; doi: 10.1007/s00339-012-7402-8
31. Morin SA, Shepherd RF, Kwok SW, et al. Camouflage and display for soft machines. Science 2012;337(6096):828–832; doi: 10.1126/science.1222149
32. Pikul JH, Li S, Bai H, et al. Stretchable surfaces with programmable 3D texture morphing for synthetic camouflaging skins. Science 2017;358(6360):210–214; doi: 10.1126/science.aan5627
33. Chen B, Bai Y, Xiang F, et al. Stretchable and transparent hydrogels as soft conductors for dielectric elastomer actuators. J Polym Sci Part B Polym Phys 2014;52(16):1055–1060; doi: 10.1002/polb.23529
34. Lee YR, Kwon H, Lee DH, et al. Highly flexible and transparent dielectric elastomer actuators using silver nanowire and carbon nanotube hybrid electrodes. Soft Matter 2017;13(37):6390–6395; doi: 10.1039/C7SM01329A
35. Shian S, Diebold RM, Clarke DR. Tunable lenses using transparent dielectric elastomer actuators. Opt Express 2013;21(7):8669–8676; doi: 10.1364/OE.21.008669
36. Zhang P, Wyman I, Hu J, et al. Silver nanowires: Synthesis technologies, growth mechanism and multifunctional applications. Mater Sci Eng B 2017;2231–23; doi: 10.1016/j.mseb.2017.05.002
37. Yun S, Niu X, Yu Z, et al. Compliant silver nanowire-polymer composite electrodes for bistable large strain

actuation. Adv Mater 2012;24(10):1321–1327; doi: 10.1002/adma.201104101
38. Pyo JB, Kim BS, Park H, et al. Floating compression of Ag nanowire networks for effective strain release of stretchable transparent electrodes. Nanoscale 2015;7(39):16434–16441; doi: 10.1039/C5NR03814F
39. Sun Y. Silver Nanowires-unique templates for functional nanostructures. Nanoscale 2010;2(9):1626–1642; doi: 10.1039/C0NR00258E
40. Kholid FN, Huang H, Zhang Y, et al. Multiple electrical breakdowns and electrical annealing using high current approximating breakdown current of silver nanowire network. Nanotechnology 2015;27(2):025703; doi: 10.1088/0957-4484/27/2/025703
41. Herring P. The Biology of the Deep Ocean. Oxford University Press: New York, NY, USA; 2002.
42. Kaltseis R, Keplinger C, Koh SJA, et al. Natural rubber for sustainable high-power electrical energy generation. RSC Adv 2014;4(53):27905–27913; doi: 10.1039/C4RA03090G
43. Tan MWM, Thangavel G, Lee PS. Enhancing dynamic actuation performance of dielectric elastomer actuators by tuning viscoelastic effects with polar crosslinking. NPG Asia Mater 2019;11(1):62; doi: 10.1038/s41427-019-0147-5
44. Sun H, Liu X, Yu B, et al. Simultaneously improved dielectric and mechanical properties of silicone elastomer by designing a dual crosslinking network. Polym Chem 2019;10(5):633–645; doi: 10.1039/C8PY01763H
45. Qiu Y, Zhang E, Plamthottam R, et al. Dielectric elastomer artificial muscle: materials innovations and device explorations. Acc Chem Res 2019;52(2):316–325; doi: 10.1021/acs.accounts.8b00516
46. Blough T, Colin SP, Costello JH, et al. Ontogenetic changes in the bell morphology and kinematics and swimming behavior of rowing medusae: The special case of the limnomedusa liriope tetraphylla. Biol Bull 2011;220(1):6–14; doi: 10.1086/BBLv220n1p6

Address correspondence to:
Hui Huang
Singapore Institute of Manufacturing Technology
*Agency for Science, Technology and Research (A*STAR)*
138634
Singapore

E-mail: hhuang@simtech.a-star.edu.sg

Jian Zhu
School of Science and Engineering
Chinese University of Hong Kong at Shenzhen
Shenzhen 518172
China

E-mail: zhujian@cuhk.edu.cn